

## Article

# Onset of Alveolization Processes in Sandstones Exposed to Salt Weathering

Marco Ludovico-Marques <sup>1,\*</sup>  and Carlos Chastre <sup>2</sup> <sup>1</sup> Instituto Politécnico de Setúbal, ESTBarreiro, RESILIENCE, 2839-001 Lavradio, Portugal<sup>2</sup> CERIS, Department of Civil Engineering, NOVA School of Science and Technology, Universidade NOVA de Lisboa, 2829-516 Caparica, Portugal; chastre@fct.unl.pt

\* Correspondence: marco.marques@estbarreiro.ips.pt

**Abstract:** Sandstones of the Lourinhã Formation were studied. Alveolization is the major form of weathering on the façades of monuments near Peniche in the western region of Portugal. Salt weathering is an important cause of this degradation form. Stones of specimens, similar to those found in these ancient buildings, were used for an experimental program of artificial salt ageing through the use of sodium chloride, calcium chloride, and sodium sulfate solutions, all at 10% (*w/w*). Salt weathering follow-up was carried out viz. the assessment of the degradation effect on these specimens of lower values of porosity under crystallization–dissolution cycles. Sodium chloride and sodium chloride with calcium sulfate were the more deleterious solutions, causing failure of the specimens after at least 40 cycles of immersion/drying. Surfaces of the sandstone specimens of variety A showed the onset of the alveolization form due to the use of a saline solution of sodium chloride with calcium sulfate.

**Keywords:** sandstones; cultural heritage; saline solutions; salt effect; alveolization pattern



**Citation:** Ludovico-Marques, M.; Chastre, C. Onset of Alveolization Processes in Sandstones Exposed to Salt Weathering. *Buildings* **2024**, *14*, 706. <https://doi.org/10.3390/buildings14030706>

Academic Editor: Humberto Varum

Received: 24 December 2023

Revised: 28 February 2024

Accepted: 29 February 2024

Published: 6 March 2024



**Copyright:** © 2024 by the authors. Licensee MDPI, Basel, Switzerland. This article is an open access article distributed under the terms and conditions of the Creative Commons Attribution (CC BY) license (<https://creativecommons.org/licenses/by/4.0/>).

## 1. Introduction

According to the terminology of degradation patterns in UNI1182 (2006) [1], Henriques et al. (2004) [2], Fitzner and Heinrichs (2004) [3], and Fitzner (2008) [4] considered for built heritage, these are currently known as granular disintegration, sanding, powdering, detachment, flaking and exfoliation, chipping, pitting, and alveolization.

Alveolization is the main weathering pattern on the sandstone blocks on the façades of historical buildings in Atouguia da Baleia Village, near Peniche in the western region of Portugal, which is mainly due to salt weathering progression. This work intends to contribute to the knowledge of the salt-weathering effect on these heritage stones with lower values of porosity and permeability.

Several authors have studied the mechanisms of degradation due to salts, which are mainly physical. The important works that must be introduced are: Wellman and Wilson (1965) [5], Rodriguez-Navarro et al. (1999) [6], and Scherer (1999, 2000, 2004) [7–9].

Wellman and Wilson (1965) [5] established that crystallization occurs when a saturated salt solution fills the small pores and large pores of a porous material through the drying of water or temperature variation. Larger crystals will develop in the larger pores with the loss of small crystals in the small pores and this process, according to Wellman and Wilson (1965), causes cavernous weathering. The occurrence of salt weathering is easier when the microporous zones of rocks are between the large pores.

Rodriguez-Navarro et al. (1999) [6] demonstrated the interdependence between the action of salts and wind in the formation of alveolization. These authors conducted experimental studies that allowed them to reproduce incipient alveolization in samples of monolithic limestone of Monks Park that were exposed to the action of wind and the crystallization of salts. They reported that a heterogeneous wind flow over a surface

promoted the development of salts between the grains by evaporation in small cavities, distributed randomly. The decrease in air pressure in these cavities caused an increase in wind speed and a higher evaporation rate. Cooling observed during the evaporation of the solution in the cavities led to a larger and faster granular disintegration of the stone materials therein. According to these authors, the supersaturation of the sodium sulfate solution and the consequent appearance of crystallization pressures were responsible for the occurrence of these forms of degradation. The former occurred inside the smaller pores and not in the larger ones due to the suction of the saturated solution from larger pores to micrometer-sized pores as evaporation progressed and a critical supersaturation was obtained in smaller ones.

These authors pointed out that the mechanisms of alteration by saline crystallization in porous materials are generally recognized as essentially being physical mechanisms.

Scherer (1999, 2000, 2004) [7–9] stated that the small openings of pores (nanometer-sized) held large crystal growth and when the maximum pressure is exerted perpendicular to the confining surface of pores, it can be higher than the tensile stress when the supersaturation is enough to cause failure.

Viles (2005) [10] concluded that an integrative model of the mechanisms responsible for alveolization weathering was missing, despite at least ninety papers regarding alveolization and tafionization being published in the last eighty years, as reported in Mustoe (1982) [11] and Goudie and Viles (1997) [12]. However, it was possible to establish a link between the concept of salt diffusion cells by McBride and Picard (2004) [13], the development model of a single cave by Huinink et al. (2004) [14], and the development of a set of caves in an outcrop (Turkington and Phillips, 2004) [15], which allowed different relevant explanations to different scales. Viles (2005) [10] also stated that these three papers complemented each other and illustrated the scientific approach to be followed: field studies, laboratory, and computer modeling.

Concerning the characterization of rock materials, the main method of research that Viles (2005) [10] predominantly focused on was the study of the physical properties related to the transportation of water and salt solutions. In fact, the model presented by Huinink et al. (2004) [14] essentially considered these physical parameters and did not contemplate the crystallization pressures or hydration, nor the effect of temperature on the expansion of the salts. Although Huinink et al. (2004) [14] allowed to carry out a computational simulation, it was a physical model that intended to explain, according to the authors, the appearance of cavities in a qualitative way.

Viles (2005) [10] carried out artificial salt crystallization ageing on samples of limestones harvested in Europe. The author performed 10 cycles of 24 h immersion in sodium sulfate, drying at 40 °C and 50% RH. Goudie (1999) [16] described the characteristics of the porous space, based on the coefficient of saturation and microporosity, as being important. He stressed the need to determine the pore size distribution and its interconnectivity by mercury intrusion porosimetry (PIM).

Robinson and Williams (2000) [17] used quartzitic sandstones (Elbasandstein) to perform artificial ageing through salt crystallization. These authors performed 35 cycles of 2 h immersion in saturated and salt solutions, drying for 69 h at 50 °C, and cooling for 1 h at room temperature. In the end, they proceeded to desalination. They assessed through the loss of mass the effect of saturated solutions of halite and gypsum salts, isolated and combined, on the sandstone specimens. Regarding later solutions, considering the volume ratios of 1:1 and 3:1, the effect was more deleterious than in each of the solutions per se, with special focus on the last proportion. In re-saturated solutions, the effect was higher in the ratio of 1:1, decreasing to 1:3 and to 3. Gypsum only enhanced the effect of halite when it was in a solution with NaCl and  $\text{CaSO}_4 \cdot 2\text{H}_2\text{O}$ . Honeyborne, cited in Evans (1970) [18], had already mentioned that a mixture of NaCl and  $\text{CaSO}_4$  had much more effect on the sandstones than each of the isolated solutions.

Ludovico-Marques and Chastre (2012) [19] carried out monotonic and cyclic uniaxial compression tests on sandstone samples after sodium chloride crystallization ageing tests and assessed the compressive mechanical behavior of the sandstones during accelerated ageing.

Flatt et al. (2014) [20] presented the results of the sodium sulfate effect on Portland limestone when the pore saturation and the crystallization pressure varied under control and reported that a failure criterion based on strain energy had the potential to predict the occurrence of damage.

Flatt et al. (2017) [21] later presented a simple conceptual model for the development of salt damage in porous materials, comprising an initial stage responsible for inducing the movement of ions and the transport and accumulation of salt in the pores without knowable damage until the damage onset (i.e., a critical point before the propagation phase), where in the latter, material degradation occurred, showing a loss of strength and cohesiveness.

Bruthans et al. (2018) [22] carried out laboratory experiments and field measurements on quartz marine sandstones with a more occurrent pore size range of 20 to 100  $\mu\text{m}$ , with the occurrence of pores with a diameter lower than 10  $\mu\text{m}$  higher in the lips of the honeycomb pattern than in the backwalls. They found that the honeycomb backwalls were reached by the evaporation front from the capillary zone when the water was under a low water flow rate, ensuring the lips dry. Salt weathering occurs mostly at the evaporation depth, breaking the rock and extending the cavities.

Belfiore et al. (2021) [23] studied the historic city center of Syracuse. The calcarenites of its building materials that showed severe alveolization, according to these authors, were linked to a micrite dominated matrix where micropores were predominant. Open porosity values of these stones varied from 14–24% to 30%, and small pores in the size range of 0.01–8  $\mu\text{m}$  were the most frequent and most favorable to salt weathering.

Oguchi and Yu (2021) [24] performed a review of the salt weathering effect on building stones based on the literature covering two centuries and concluded that more developed theories should be published to contribute to the understanding of the related weathering mechanisms.

Galanaki et al. (2022) [25] carried out accelerated salt ageing tests of sodium chloride through total immersion, for 60 days, on four different biocalcarenes and a calcitic sandstone. The authors concluded that the pores' percentage of radii higher than 10  $\mu\text{m}$  had an important role regarding the resistance of the samples to NaCl crystallization damage.

Recent specific experimental studies published regarding the causes of alveolization on sandstones are scarce, and other relevant papers are also reported because they illustrate degradation features due to the effect of salts.

Conservation works suitable for deteriorated sandstones showing the degradation patterns found on the cultural built heritage studied encompass consolidation treatments of the exposed stone surfaces.

Considering that ethyl silicate applications have generally shown good results regarding the conservation of sandstones, two commercially available tetraethoxysilane (TEOS) products were tested on sandstone specimens in laboratory: Tegovakon V (TG) and Redur 420 (R).

This first stage of consolidation works intended to assess the viability of future TEOS applications on these stone walls. Ludovico-Marques and Chastre (2014, 2016) [26,27] carried out experimental research on sandstone specimens similar to the stones of variety M in the monument, with circa 3–5 times the porosity values of varieties B and A. These products were applied by an initial immersion and capillarity procedure, followed by full immersion. A solvent evaporation time of 2 months took place and the samples retained a dry residue of about 23.5% of R and 38.5% of TG in the sandstone samples from around a 5% of mass content absorbed. The performance of R was better than that of the TG applications, despite the consolidation effect of TG was higher, due to its lower durability during the accelerated artificial ageing sodium chloride crystallization tests.

Using the same treatment procedures on the specimen A and B varieties, the mass content absorbed in the former samples was lower than 0.5%, and in the latter, it was circa 1%. Regarding specimens of typology B, the values of dry residue were about 17% in TG

and around 10% in the R-treated specimens, and the evaporation of solvents lasted more than 2 months. The specimens of variety A showed values of dry residue lower than 2%. The consolidation effect on specimens of the B variety was minor, and not significant on samples of the A variety.

Considering that the consolidation effect was not meaningful on treated samples of the A+B lithotype and the performance of TG applications was not good due to the lower durability obtained on variety M, future consolidating treatments are not recommended by the authors in the conservation works of these stones of the monument. Additionally, due to the location of St. Leonard's Church close to the sea, this is a major source of sodium chloride that is linked to the widespread alveolization through capillary and salt mist transportation. This monument was built in the 12th century, where salt weathering has progressed for more than 800 years to today. Figure 1 illustrates representative alveolization forms shown on a block of B variety sandstone in the south portal. As it is visible, alveolization is in an early stage in this lithotype.

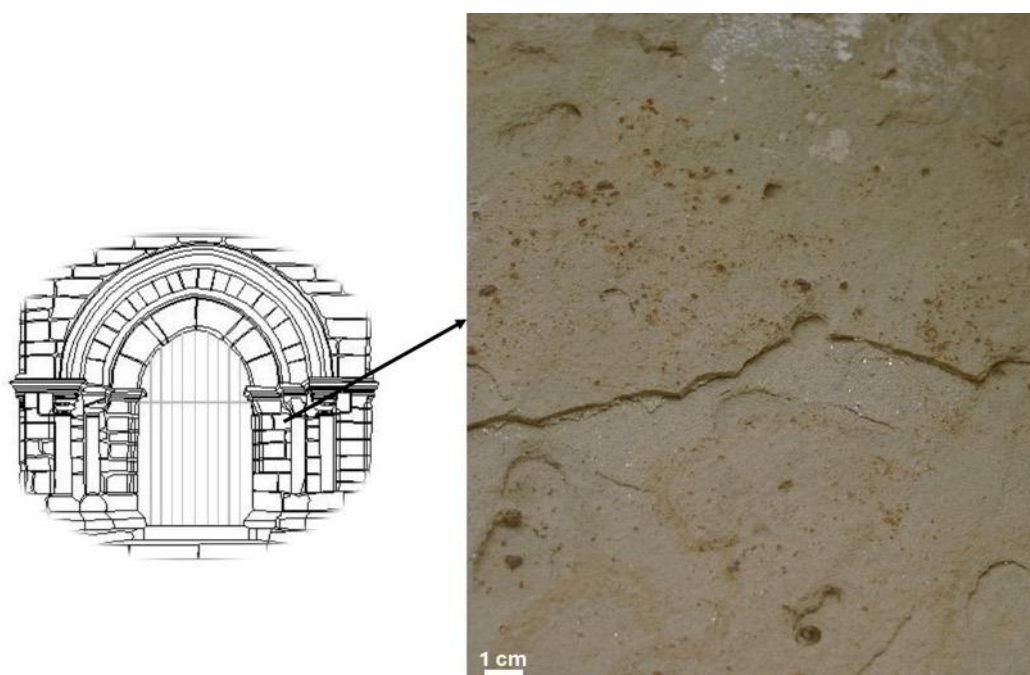


**Figure 1.** Representative alveolization forms on a sandstone block of the B variety located at the south portal of St. Leonard's Church.

Wheeler (2005), citing Butlin et al. (2002) [28], showed detailed data of consolidating treatments through the application of a MTMOS product, Brethane, on cultural heritage sandstones (e.g., in castles and abbeys sites) with higher values of porosity. The study reported that Brethane did not perform well when the durability was assessed through the salt effect.

Prior works of conservation based on the visual inspection of facades and monitoring the weathering forms on sandstone blocks of variety B has been carried out by the authors.

The next sections will show the characterization of these stones, the experimental methodology followed and the corresponding theoretical background, the tests results, its interpretation and discussion regarding salt weathering follow-up during artificial ageing performed on heritage sandstones of lithotype A+B, and our conclusions regarding the effectiveness of the different saline solutions used in terms of triggering the onset of alveolization. Future conservation works of the monument are also recommended.

## 2. Materials and Methods

### 2.1. Characteristics of the Sandstones Studied

The authors highlight that the following results shown in this subsection were obtained from their works of experimental research performed previously.

The sandstone samples studied belong to the Lourinhã Formation and were collected in the vicinity of the surrounding walls of monuments at the village of Atouguia da Baleia. These stones are similar to those found in other cultural heritage in this area.

Ludovico-Marques and Chastre (2019) [29] reported four varieties of sandstones found in cultural heritage. These were classified as lithic arkose with carbonate cement, according to the classification of Folk (1974) [30]. The composition of lithotypes A+B and C+M are referred to in Table 1.

**Table 1.** Mineralogical and physical properties of lithotypes studied.

Properties	Lithotype A+B	
	Variety A	Variety B
Mineral composition	c.a. 34–40% of carbonates, 30–32% of quartz, 13–16% of feldspars, 4–6% of mica and 5% of lithic fragments. *	
Average size of quartz and feldspar grains (mm)	Range: 0.1–0.13 (fine-grained)	
Porosity (%)	$X_{\text{mean}}^{**} \pm \sigma^{***}$ 4.1 ± 0.4	Range: 3–8 $X_{\text{mean}} \pm \sigma$ 6.9% ± 0.5
Median pore radius (µm)	Range: 0.14–0.39	
Capillarity water absorption coefficient (kg/m <sup>2</sup> h <sup>1/2</sup> )	$X_{\text{mean}} \pm \sigma$ 0.4 ± 0.1	Range: 0.3–0.7 $X_{\text{mean}} \pm \sigma$ 0.6 ± 0.1
Drying index	$X_{\text{mean}} \pm \sigma$ 0.37 ± 0.02	Range: 0.18–0.39 $X_{\text{mean}} \pm \sigma$ 0.20 ± 0.01

\* Lithotype C+M has around 20–25% of carbonates and 40–51% quartz, 13–16% of feldspars, 4–6% of mica, and 5% of lithic fragments. \*\* Average value \*\*\* Standard deviation.

This article only considers varieties A and B.

Figure 2 shows the thin-section observations carried out through a polarizing microscope with crossed nicols. Lithotype A+B showed well-defined lineation. One major orientation of mica minerals was exhibited in the A variety, while preferred orientations were not shown in variety B.

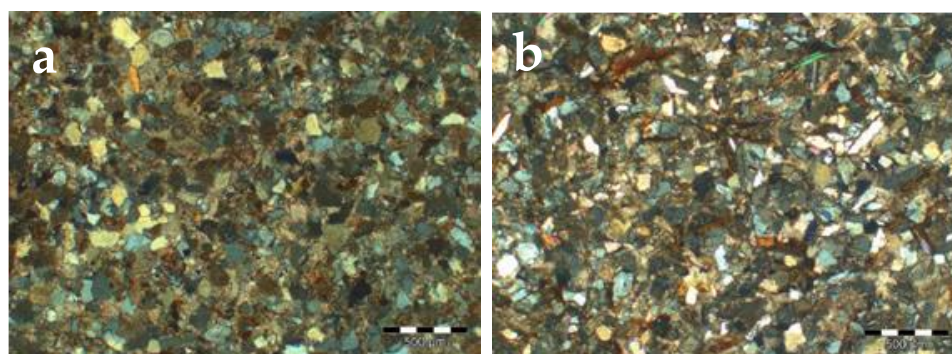


**Figure 2.** Thin-section observations carried out under a polarizing microscope (crossed nicols) for varieties (a) A and (b) B.

The counting method of thousands of points was used to perform the modal analysis that allowed us to determine the mineral composition of the lithotypes.

Table 1 shows the values obtained by the following tests performed on specimens of lithotype A+B: porosity through the Archimedes principle and capillarity water absorption according to RILEM (1980) [31]; pore size distribution (PSD) was determined by mercury intrusion porosimetry (MIP) using AutoPore IV9500 equipment; the drying index (DI) was computed as asked by the NORMAL Recommendation 29/88 [32] under laboratory conditions of  $20 \pm 2$  °C and  $55 \pm 10\%$  RH.

These are fine-grained stones with low values of porosity, water absorption, and a pore radius median ranging between values of 0.14 and 0.39  $\mu\text{m}$ .

## 2.2. Experimental Work of Salt Ageing of Stones

### 2.2.1. Introduction

The fastest modes of the degradation of porous materials are continuous cycles of wetting and the absorption of saline solutions, alternating with drying and cooling. In order to assess the durability of the materials, artificial ageing tests were carried out. These consisted of samples of materials that were wetted, through voids accessible to the water, by saline solutions for a period, after which they were submitted to drying under low RH laboratory conditions and then cooled, which also took place within a defined period and so on in repeated cycles.

### 2.2.2. Experimental Knowledge Obtained from Procedures followed on Salt Ageing Tests for Stones Prior to the Tests Carried out on Lithotype A+B

In order to carry out artificial salt crystallization ageing tests, there are standards that define the testing times and the respective temperature and humidity conditions (RILEM V.1a, b, V.2 of 1980; EN 12370) [31,33]. In general, for natural stones, immersion must take place at an ambient temperature of  $20 \pm 0.5$  °C, drying must be carried out at temperatures between 60 °C and  $105 \pm 5$  °C, and cooling also at  $20 \pm 0.5$  °C. In the case of materials treated with polymeric consolidants, the drying temperature will be 60 °C, which cannot be exceeded, otherwise degradation of the properties of these consolidating products will occur. Whenever comparative studies of salt degradation between polymer-consolidated and non-consolidated materials are attempted, tests should be carried out at 60 °C.

The number of cycles and duration of each cycle as well as each wetting/immersion, drying, and cooling phase are regulated by standards. Table 2 shows the corresponding specifications for immersion/drying and salt spray tests for natural stones as well as the procedures followed by the reported authors. Ludovico Marques and Delgado Rodrigues (2002) [34] carried out salt spray tests on volcanic tuffs. Ferreira Pinto (2002) [35] performed tests on carbonated stones. Warke et al. (2005) [36] carried out immersion/drying tests on sandstones, as did Robinson and Williams (2000) [17].

**Table 2.** Representative specifications of the test standards and conditions implemented by the reported authors.

Standard/ Author	No. of Cycles	Wetting			Drying			Cooling		
		Method	T (°C)	Time (h) Salts (conc.)	Time (h)	T (°C)	HR (%)	Time (h)	T (°C)	HR (%)
RILEM V1a (1980) [31]	15	Total immersion (NT <sup>1</sup> )	$20 \pm 0.5$	2 h Na <sub>2</sub> SO <sub>4</sub> ·10H <sub>2</sub> O (14%)	≥16	$105 \pm 5$	High (in the beginning)	Non detailed	$20 \pm 0.5$	Not referred
RILEM V1b (1980) [31]	≥15	Total immersion (A <sup>2</sup> )	$20 \pm 0.5$	2 h Na <sub>2</sub> SO <sub>4</sub> (10%)	≥19	$60 \pm 5$	High (in the beginning)	3	$20 \pm 0.5$	Not referred
RILEM V 2 (1980) [31]	≥15	Partial immersion (A <sup>2</sup> )	$20 \pm 0.5$	2 h Na <sub>2</sub> SO <sub>4</sub> (10%)	≥19	$60 \pm 5$	High (in the beginning)	3	$20 \pm 0.5$	Not referred

Table 2. Cont.

Standard/ Author	No. of Cycles	Wetting			Drying			Cooling		
		Method	T (°C)	Time (h)	Time (h)	T (°C)	HR (%)	Time (h)	T (°C)	HR (%)
				Salts (conc.)						
EN 12370 (2020) <sup>3</sup> [33]	15	Total immersion	20 ± 0.5	2 h Na <sub>2</sub> SO <sub>4</sub> ·10H <sub>2</sub> O (14%)	≥16	105 ± 5	High (in the beginning)	2 ± 0.5	20 ± 0.5	Not referred
Ludovico Marques and Delgado Rodrigues (2002) <sup>4</sup> [34]	50	Salt mist	35	10 h NaCl (180 g/L)	38	35	Not referred	Not referred	Not referred	Not referred
Ferreira Pinto (2002) <sup>4</sup> [35]	50	Salt mist	35	4 h (120 g/L) <sup>5</sup> (160 g/L) <sup>5</sup> (180 g/L) <sup>6</sup> (180 g/L) <sup>6</sup>	20 24 24 38	35	Not referred	Not referred	Not referred	Not referred
Warke et al. (2005) [36]	220	Total immersion	10–40	10 h Na <sub>2</sub> SO <sub>4</sub> (2.5%)	10	10–40	Not referred	-----	-----	-----

<sup>1</sup> Untreated; <sup>2</sup> Treatment applications; <sup>3</sup> Procedures of NP EN 12370 (2002) followed; <sup>4</sup> At the end of the tests, the referred authors carried out 19 cycles of deionized water to remobilize the salt that had accumulated inside the specimens during the previous 50 cycles; <sup>5</sup> KNO<sub>3</sub>; <sup>6</sup> NaCl.

The saline solutions most commonly used are sodium chloride in the case of salt spray tests (former EN 14147) [37] and sodium sulfate decahydrate (RILEM V.1a, b, V.2; EN 12370) [31,33].

Salt concentrations range from 10 to 14%.

For research purposes, other solutions and other concentrations may be used, as long as they are adequate for the objectives to be achieved.

Almost all the referred standards advocate the use of cubic specimens, 5 cm long. Only EN 12370 [33] indicates specimens with an edge length of 4 cm.

At the end of the test, almost all of the standards and recommendations specify that the salt absorbed by the specimens is dissolved in deionized water at room temperature, 20 ± 0.5 °C. UNI EN 16455 (2014) [38] states that the conductivity of the deionized water used for salt analysis cannot exceed 3 µS/cm.

The results can be presented in the form of a photographic record of the evolution of the surface of the specimens. The indication of the number of cycles necessary for the breakage or disintegration of the specimens to occur is also required. EN 14147 [37] specifies that this failure must be verified in at least two specimens in a standard set under study to be accepted as a criterion to end the test.

### 2.2.3. Procedures of Artificial Ageing Tests by Crystallization of Salts Performed on Lithotype A+B

The test procedures adopted within the scope of this work were selected in order to allow for the evaluation of the effect of salt solutions in inducing greater accelerated degradation of the sandstone materials studied in the 5 cm long cubic specimens.

Tests were carried out with variety A specimens in an Ascott salt spray chamber with a capacity of 450 L at the Laboratory of Durability of Structures of DEC of FCT. The same method of specimen preparation was followed as in Ludovico Marques and Delgado Rodrigues (2002) [34]: the four faces became laterally impermeable, except for the surrounding area of a centimeter of height close to the edge, starting from the top.

The product applied was SIKA's Icosit K101 epoxy resin by brushing on two coats. The specimens were placed in Petri dishes inside the fog chamber and submitted to 15 cycles of 48 h each, with 12 h of wetting by sodium chloride mist at a concentration of 10% (10 g of salt to 90 g of water) and 36 h of drying at 35 °C.

Another test was carried out with specimens of the same variety, first for 15 cycles and after for 40 cycles of 24 h each, consisting of total immersion in a glass container with 10% sodium chloride (*w/w*) for a period of two hours at room temperature in the laboratory, followed by 20 h of drying in an oven at 60 °C and 2 h of cooling.

The room conditions were a temperature of  $20 \pm 2$  °C and  $55 \pm 10\%$  RH.

Other crystallization tests of 40 cycles using the same distribution of hours between total immersion, drying, and cooling were carried out using the following solutions: decahydrate sodium sulfate solution at 10% (*w/w*) as well as sodium chloride solutions with calcium sulfate at 10% (*w/w*), distributed according to the ratio 4:1.

The experimental device is shown in Figure 3.

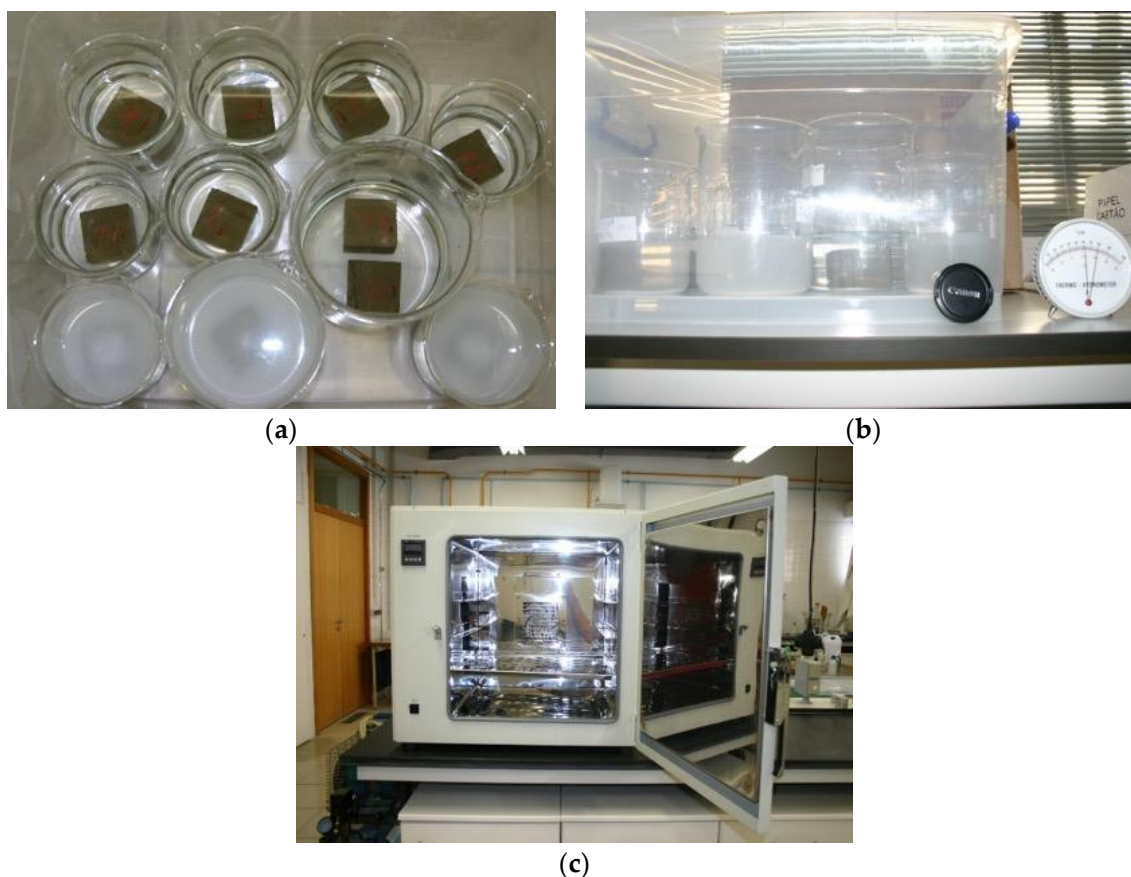


**Figure 3.** Experimental device for testing the cycles of immersion in saline solutions, drying at 60 °C, and cooling at room temperature: (a) specimens immersed in saline solutions; (b) immersion phase under controlled environment temperature; (c) ventilated oven for drying the specimens.

Sodium chloride crystallization–dissolution cycles were performed on variety B specimens inside the automatic ageing chamber described in Ludovico-Marques (2008) [39] and from Ludovico-Marques and Chastre (2012) [19]. The experimental program encompassed 60 cycles of 2 h of sample immersion within a 10% sodium chloride solution (*w/w*), 20 h of heating, and 2 h of cooling.

After the salt ageing cycles, all of the specimens used were washed with deionized water; this procedure only ended when a concentration of about 1 ppm of ions in an hour was obtained in the salt-removing water. Afterward, the samples were dried inside an oven at 60 °C and left inside a desiccator at 20 °C.

An experimental control was implemented through the immersion of specimens in deionized water and drying in an oven at 60 °C. Thermal shock by heating–cooling cycles was also performed on non-immersed specimens.

### 3. Results and Discussion

By visually comparing the specimens before and after carrying out 15 salt cycles in the salt spray chamber and in the glass container shown in Figure 3, there was a perceptible evolution only in the later samples. These specimens lost cohesion between their planar surfaces of anisotropy, rather than those that were in the salt spray chamber, as shown in Figure 4.



**Figure 4.** Aspect of specimens after salt crystallization tests by: (a) salt mist; (b) immersion/drying (left and right columns correspond to 0 and 15 cycles).

In these tests, the deterioration effect of the stone materials was more accelerated after the cycles of immersion in saline solution and drying at 60 °C, than after cycles of wetting by salt mist and drying at 35 °C. We decided to proceed with the test of immersion/drying cycles also comprising the saline solutions of decahydrated sodium sulfate at 10% (*w/w*) and the mixture of sodium chloride and calcium sulfate at 10% (*w/w*), distributed in the ratio of 4:1.

Figure 5 shows the aspect of the specimens after the tests carried out over 40 cycles. A higher degradation effect was found for the sodium chloride crystallization and dissolution cycles. These specimens showed a loss of cohesion with complete separation of laminations, reaching failure (Figure 6). The saline mixture was responsible for the same phenomenon but with lower effect (Figure 7) and caused erosion to the surface of the specimens due to the action of calcium sulfate (Figures 8 and 9). The experimental results observed in Figures 5, 6, 8 and 10 revealed that the sodium chloride solution and the mixture solution were more deleterious to the variety A sandstone during the 40 cycles of crystallization and dissolution than the sodium sulfate solution. The tensile stresses developed during the crystallization of NaCl caused a significant spacing between the laminations, which was more expressive than that observed in the crystallization of the sodium sulfate system (Figure 10).

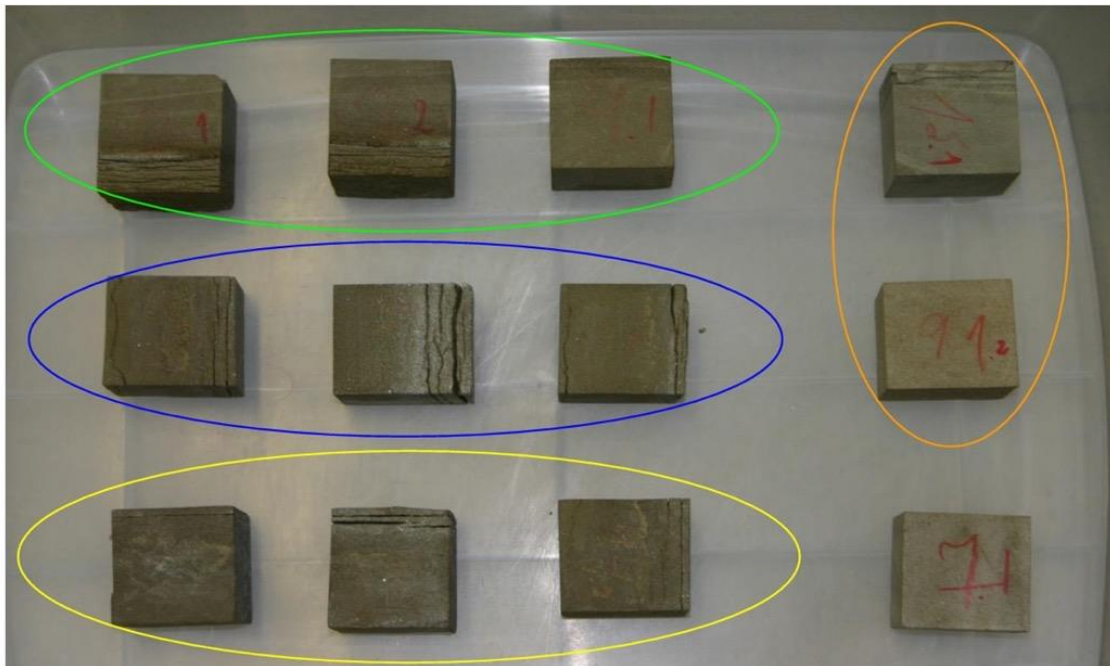


**Figure 5.** Features of the specimens after 40 cycles of crystallization–dissolution: inside the green oval, they were in the sodium sulfate solution; in the blue oval, they were in the sodium chloride solution; inside the yellow oval, they were in the sodium chloride and calcium sulfate solution; in the orange oval, they were only under the effect of deionized water; without oval, this was only under the influence of temperature.



**Figure 6.** Detailed aspects of three representative specimens before and after the sodium chloride crystallization–dissolution test.



**Figure 7.** Detailed aspects of three representative specimens before and after the crystallization and dissolution cycles of sodium chloride and calcium sulfate solution.

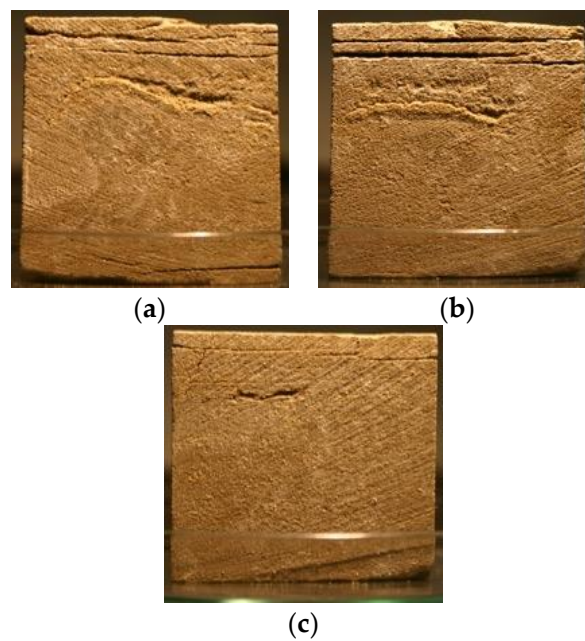


**Figure 8.** Detailed aspects of three different faces of representative specimen 96.2 after 40 cycles of crystallization and dissolution cycles using sodium chloride and calcium sulfate solution: (a–c) grooves form as superficial erosion.

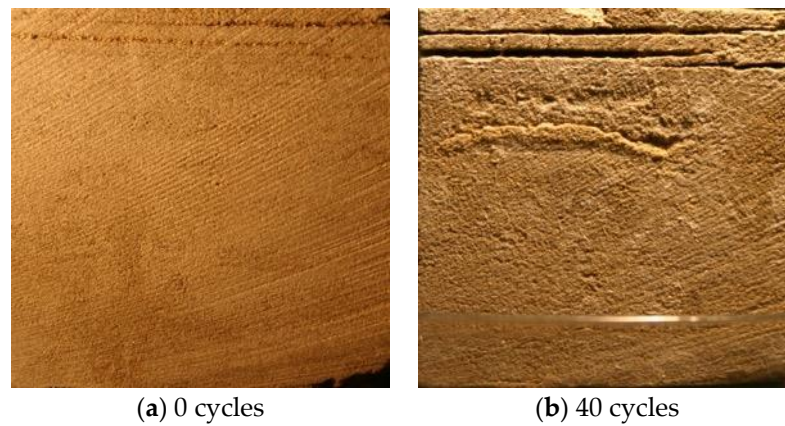


**Figure 9.** Magnification of specimen 96.2 (a) sound sample before salt crystallization ageing test (b) cavity shown after 40 cycles (presumed start of alveolization weathering).



**Figure 10.** Detailed aspects of three representative specimens before and after the sodium sulfate crystallization and dissolution cycles.

The specimens after 40 cycles of immersion in deionized water and drying at 60 °C did not show minimal significant differences compared to their state before the test was conducted. It should be noted that one of the specimens already showed a fracture near one of the faces before the test was carried out and even so, at the end of the test, no evolution occurred, as can be inferred from Figure 11. Furthermore, the specimen after 40 cycles of heating and cooling did not present any visible variation (Figure 12).

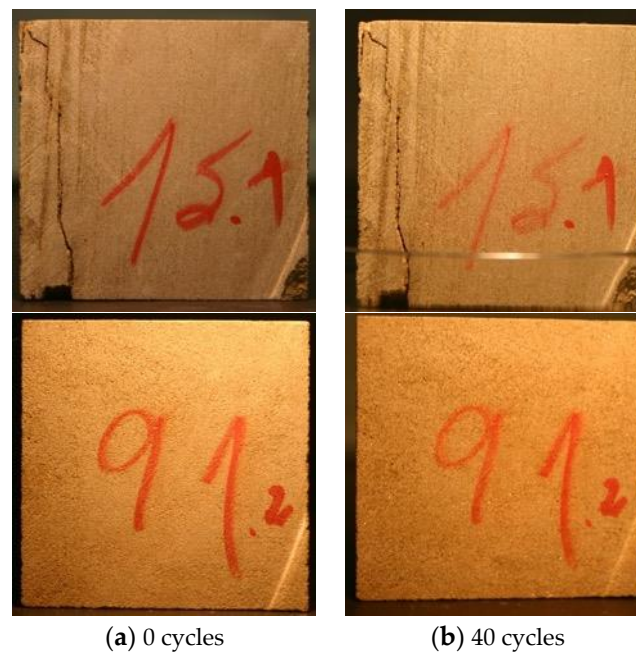


**Figure 11.** Detailed aspects of the specimens before and after cycles of immersion in deionized water and drying.

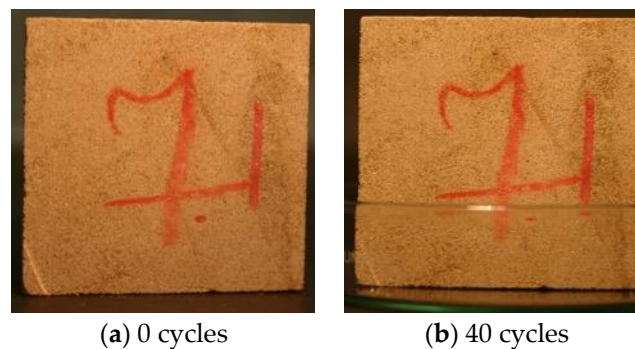


**Figure 12.** Detailed aspects of the specimen before and after cycles of heating and cooling.

These results reveal the importance of the degradation effect caused on sandstones due to the implementation of experimental cycles of sodium chloride crystallization and dissolution.

The variety B specimens were inserted on one of the trays in a climatic chamber that carried out 60 artificial ageing tests by sodium chloride crystallization and dissolution, following the procedures referred to in Section 2.2.3. Sodium chloride exhibited a more deleterious effect on the variety A specimens and the onset of alveolization was found through artificial crystallization–dissolution ageing tests based on the use of the sodium chloride and calcium sulfate solution. Therefore, only sodium chloride crystallization–dissolution ageing tests were carried out on variety B specimens.

Figure 13 shows the macroscopic observations of faces of a representative specimen, which was selected to illustrate the degradation process during the test. The deterioration of variety B was essentially due to the occurrence of fractures along some planes of discontinuous lineations; after the 40th cycle, chipping developed that later detached and reliefs appeared. Alveolization forms in Figure 1 and degradation features in Figure 13 showed a slight resemblance, however, it is not possible to conclude that the latter are alveolization patterns.

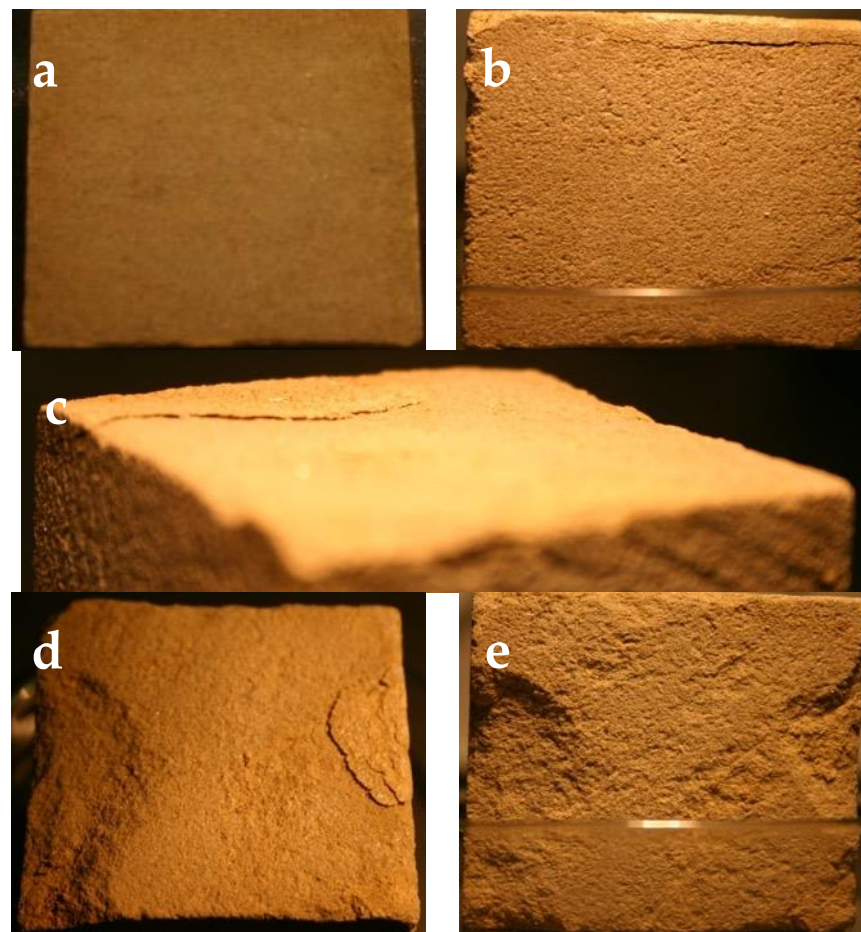


**Figure 13.** Aspects of a representative specimen of variety B under the salt crystallization–dissolution test during 60 cycles. (a) Top face before testing. (b) Same face showing a fracture and irregularity of the edges after 40 cycles. (c) Detail of the fracture on its surface, the face adjacent to the top face, after 40 cycles. (d) Formation of chipping due to the development of the referred fracture and the occurrence of another after 50 cycles. (e) Chipping, detachment, and reliefs found on this face after 60 cycles.

Several authors have reported that ageing performed in laboratory conditions is much more effective through the use of individual saline solutions of sodium sulfate, magnesium sulfate, and sodium carbonate than sodium chloride and calcium sulfate solutions (Pedro, 1957; Kwaad, 1970; Goudie, 1974; Sperling and Cooke, 1985) [40–43]. However, the experimental results shown in Figures 5, 6, 8 and 10 revealed that the sodium chloride solution and the mixture solution were more deleterious to variety A sandstone during the 40 cycles of crystallization and dissolution than the sodium sulfate solution. The tensile stresses developed during the crystallization of NaCl caused a significant spacing between laminations, which was more expressive than those recorded when crystallization of the sodium sulfate occurred (Figure 10).

Sodium chloride solutions with calcium sulfate at 10% (*w/w*), distributed according to the ratio 4:1, were not used by Robinson and Williams (2000) [17], who studied the effect of different proportions. The cavity in the specimen shown in Figure 9b can be considered the beginning of alveolization weathering. This is a contribution of this experimental work: a specific distribution of sodium chloride and calcium sulfate in the salt solution triggers the onset of alveolization.

Rodriguez-Navarro et al. (1999) [6] used Monks Park oolitic limestone with a median pore radius of 0.25  $\mu\text{m}$  and a mean porosity of 22.7% obtained by MIP. A sodium sulfate saturated solution was applied. In the laboratory, values of *T* were  $20 \pm 2$  °C and the

RH was  $50 \pm 10\%$ , similar to the present work conditions. The former authors obtained incipient alveoles on the specimens' surfaces due to the crystallization of salt under wind perpendicular to the slab's surface. In the present work, the range of the median sandstones' pore radius was  $0.14\text{--}0.39\ \mu\text{m}$ , similar to the corresponding value reported by Rodriguez-Navarro et al. (1999) [6]. The experimental results of both authors converged to values of the median pore radius of stones studied that were lower than  $0.5\ \mu\text{m}$ , and considering this parameter of pore size distribution, it can play an important role or at least facilitate salt weathering progression toward the onset of alveolization. Punuru et al. (1990) [44] also found that the presence of a large volume of narrow capillaries, with a size less than  $0.5\ \mu\text{m}$ , in specimens from rocks of the Egyptian Great Sphinx was deleterious. Long lasting solutions inside pores combined with evaporation processes will develop permanent crystallization pressures. However, the authors of the present paper recognize that alveolization does not only depend on the latter processes described. The action of wind and evaporation processes related to the former are also major causes of the weathering of stones.

#### 4. Conclusions

The facades of St. Leonard's Church show blocks of sandstone of variety B, with alveolization forms in the early stage of weathering. An experimental study regarding salt weathering by artificial salt crystallization and dissolution ageing cycles was carried out on sandstone specimens. The saline solutions used were sodium chloride, a sodium chloride and calcium sulfate mixture in the ratio of 4:1, and sodium sulfate, all at 10% (*w/w*). The results showed a higher effect of salt weathering on the lower porosity values of the variety A stone of the Lourinhã Formation, with both sodium chloride solutions effectiveness regarding the degradation of the sandstone specimens. It was not possible to cause weathering by salt mist and only the devices that functioned through immersion in saline solutions, drying at  $60\ ^\circ\text{C}$ , and cooling at  $20\ ^\circ\text{C}$  were successful at carrying out a minimum of 40 cycles. The onset of alveolization was reached on the surfaces of the variety A sandstone specimens, linked to the saline solution of sodium chloride with calcium sulfate in the ratio of 4:1. Chipping, detachment, and reliefs found on the variety B specimens after 60 cycles of crystallization and dissolution ageing cycles of sodium chloride were carried out inside an automatic chamber, were not complete alveolization patterns despite their slight resemblance. The onset of alveolization obtained was related to the value of the parameter for the median radius of pores being lower than  $0.5\ \mu\text{m}$ . This parameter seems at least to ease the weathering progress of salt. Future research works will be conducted in order to deepen studies regarding the influence of porosity on the decay of sandstones by alveolization.

The consolidation effect was not significant on the treated samples of the A+B lithotype with two TEOS products, TG and R. Neither performance was good due to the lower durability obtained. The same type of problems occurred with the MTMOS applications, according to the data found in the literature. Future conservation works of these stones should be based on visual inspection and monitoring the evolution of weathering.

**Author Contributions:** M.L.-M. developed the experimental program; M.L.-M. and C.C. analyzed the data, discussed the results, and contributed to the writing of the paper. All authors have read and agreed to the published version of the manuscript.

**Funding:** This research received no external funding.

**Data Availability Statement:** The original contributions presented in the study are included in the article, further inquiries can be directed to the corresponding author.

**Conflicts of Interest:** The authors declare no conflicts of interest.

#### References

1. UNI 11182; Beni Culturali—Materiali Lapidei Naturali ed Artificiali—Descrizione Della Forma di Alterazione—Termini e definizioni. UNI: Reggio di Calabria, Italy, 2006.

2. Henriques, F.; Delgado Rodrigues, J.; Aires-Barros, L.; Proença, N. *Materiais Pétreos e Similares. Terminologia das Formas de Alteração e Degradação. Patologia e Reabilitação da Construção*; LNEC: Lisboa, Portugal, 2004; Volume 2, p. 39.
3. Fitzner, B.; Heinrichs, K. *Photo Atlas of Weathering Forms on Stone Monuments*; Geological Institute, RWTH Aachen University—Working Group Natural Stones and Weathering: Aachen, Germany, 2004; 24p.
4. Fitzner, B. *Illustrated Glossary on Stone Deterioration Patterns. Monuments and Sites XV*; ICOMOS International Scientific Committee for Stone (ISCS): Paris, France, 2008.
5. Wellman, H.; Wilson, A. Salt weathering, a neglected geological erosive agent in coastal and arid environments. *Nature* **1965**, *4976*, 1097–1098. [[CrossRef](#)]
6. Rodriguez-Navarro, C.; Dohene, E.; Sebastian, E. Origins of honeycomb weathering: The role of salts and wind. *Bull. Geol. Soc. Am.* **1999**, *111*, 1250–1255. [[CrossRef](#)]
7. Scherer, G. Crystallization in pores. *Cem. Concr. Res.* **1999**, *29*, 1347–1358. [[CrossRef](#)]
8. Scherer, G. Stress from crystallization of salt in pores. In Proceedings of the 9th International Congress on Deterioration and Conservation of Stone, Venice, Italy, 19–24 June 2000; pp. 187–194.
9. Scherer, G. Stress from crystallization of salt. *Cem. Concr. Res.* **2004**, *34*, 1613–1624. [[CrossRef](#)]
10. Viles, H. Self-organized or disorganized? Towards a general explanation of cavernous weathering. *Earth Surf. Process Landf.* **2005**, *30*, 1471–1473. [[CrossRef](#)]
11. Mustoe, G. The origin of honeycomb weathering. *Bull. Geol. Soc. Am.* **1982**, *93*, 108–115. [[CrossRef](#)]
12. Goudie, A.; Viles, H. *Salt Weathering Hazards*; John Wiley and Sons: Chichester, UK, 1997; 241p.
13. McBride, E.; Picard, M. Origin of honeycombs and related weathering forms in Oligocene Macigno Sandstone, Tuscan coast near Livorno, Italy. *Earth Surf. Process Landf.* **2004**, *29*, 713–735. [[CrossRef](#)]
14. Huinink, H.; Pel, L.; Kopinga, K. Simulating the growth of Tafoni. *Earth Surf. Process Landf.* **2004**, *29*, 1225–1233. [[CrossRef](#)]
15. Turkington, A.; Phillips, J. Cavernous weathering, dynamical instability and self-organization. *Earth Surf. Process Landf.* **2004**, *29*, 665–675. [[CrossRef](#)]
16. Goudie, A. Experimental salt weathering of limestones in relation to rock properties. *Earth Surf. Process Landf.* **1999**, *24*, 715–724. [[CrossRef](#)]
17. Robinson, D.; Williams, R. Experimental weathering of sandstone by combinations of salts. *Earth Surf. Process Landf.* **2000**, *25*, 1309–1315. [[CrossRef](#)]
18. Evans, I. Salt crystallization and rock weathering: A review. *Rev. Geomorph Dynam* **1970**, *XIX*, 153–177.
19. Ludovico-Marques, M.; Chastre, C. Effect of salt crystallization ageing on the compressive behavior of sandstone blocks in historical buildings. *Eng. Fail. Anal.* **2012**, *26*, 247–257. [[CrossRef](#)]
20. Flatt, R.; Caruso, F.; Sanchez, A.; Scherer, G. Chemomechanics of salt damage in stone. *Nat. Commun.* **2014**, *5*, 4823. [[CrossRef](#)] [[PubMed](#)]
21. Flatt, R.; Mohamed, N.; Caruso, F.; Derluynd, H.; Desarnaude, J.; Lubelli, B.; Espinosa-Marzal, R.; Pel, L.; Rodriguez-Navarro, C.; Scherer, G.; et al. Predicting salt damage in practice: A theoretical insight into laboratory tests. *Rilem Tech. Lett.* **2017**, *2*, 108–118. [[CrossRef](#)]
22. Bruthans, J.; Filippi, M.; Slavík, M.; Svobodová, E. Origin of honeycombs: Testing the hydraulic and case hardening hypotheses. *Geomorph* **2018**, *303*, 68–83. [[CrossRef](#)]
23. Belfiori, C.; Calabrò, C.; Ruffolo, S.; Ricca, M.; Török, A.; Pezzino, A.; La Russa, M. The susceptibility to degradation of stone materials used in the built heritage of the Ortygia island (Syracuse, Italy): A laboratory study. *Int. J. Rock. Mech. Min. Sci.* **2021**, *146*, 104877. [[CrossRef](#)]
24. Oguchi, C.; Yu, S. A review of theoretical salt weathering studies for stone heritage. *Prog. Earth and Planet. Sci.* **2021**, *8*, 32. [[CrossRef](#)]
25. Galanaki, N.; Delegou, E.; Bris, T.; Moropoulou, A. Accelerated ageing tests of sodium chloride for the evaluation of stones durability to salt crystallization: A comparative study of selected restoration lithotypes. *Dev. Built Environ.* **2022**, *11*, 100081. [[CrossRef](#)]
26. Ludovico-Marques, M.; Chastre, C. Effect of consolidation treatments on mechanical behaviour of sandstone. *Constr. Build Mater.* **2014**, *70*, 473–482. [[CrossRef](#)]
27. Ludovico-Marques, M.; Chastre, C. Durability assessment of consolidation effect on sandstone monuments. In Proceedings of the 41th IAHS World Congress of Housing, Sustainability and Innovation for the Future, Albufeira, Portuga, 13–16 September 2016. 10p.
28. Wheeler, G. *Alkoxysilanes and the Consolidation of Stone. Research in Conservation*; The Getty Conservation Institute: Los Angeles, CA, USA, 2005.
29. Ludovico-Marques, M.; Chastre, C. Prediction of stress–strain curves based on hydric non-destructive tests on sandstones. *Materials* **2019**, *12*, 3366. [[CrossRef](#)] [[PubMed](#)]
30. Folk, R. *Petrology of Sedimentary Rocks*; Hemphill Publishing: Austin, TX, USA, 1974; p. 184.
31. Rilem. Recommended tests to measure the deterioration of stone and to assess the effectiveness of treatment methods. *Mater. Const. Bourdais-Dunoud* **1980**, *13*, 175–253.
32. *NORMAL-29/88*; Misura dell’Indice di Ascugamento (Drying Index). Alterazioni dei Materiali Lapidei e Trattamenti Conservativi—Proposte per l’Unificazione dei Metodi Sperimentali di Studio e di Controllo. CNR-ICR: Rome, Italy, 1991.

33. EN 12370; Natural Stone Test Methods-Determination of Resistance to Salt Crystallization. CEN: Brussels, Belgium, 2020.
34. Ludovico-Marques, M.; Delgado-Rodrigues, J. Consolidation of Volcanic Tuffs. Some physical and mechanical properties. In Proceedings of the EUROCK 2002 International Workshop on Volcanic Rocks, Funchal, Portugal, 25–28 November 2002; pp. 37–44.
35. Ferreira Pinto, A. Conservação de Pedras Carbonatadas. Estudo e Selecção de Tratamentos. Ph.D. Thesis, Universidade Técnica de Lisboa, Lisboa, Portugal, 2002.
36. Warke, P.; McKinley, J.; Smith, B. Variable weathering response in sandstone: Factors controlling decay sequences. *Earth Surf. Process Landf.* **2005**, *31*, 715–735. [[CrossRef](#)]
37. EN 14147; Natural Stone Test Methods-Determination of Resistance to Ageing by Salt Mist. European Committee for Standardization: Brussels, Belgium, 2003.
38. UNI EN 16455; Conservazione dei Beni Culturali—Dissoluzione e Determinazione di Sali Solubili Nelle Pietre Naturali e Relativi Materiali in Uso e Provenienti dal Patrimonio Culturale. UNI: Reggio di Calabria, Italy, 2014.
39. Ludovico-Marques, M. Contribution to the Knowledge of the Effect of Crystallization of Salts in the Weathering of Sandstones. Application to the Built Heritage of Atougua da Baleia. Ph.D. Thesis, Universidade NOVA de Lisboa, Lisbon, Portugal, 2008. (In Portuguese)
40. Pedro, G. Mécanisme de la désagrégation du granite et de la lave de Volvic sous l' influence des sels de cristallisation. *Compt Rendu Acad Sci. Paris* **1957**, *245*, 333–335.
41. Kwaad, F. *Experiments on the Disintegration of Granite by Salt Action*; University Amsterdam Fysisch Geografisch en Bodemkundig Laboratorium Publicatie: Amsterdam, The Netherlands, 1970; Volume 16, pp. 203–217.
42. Goudie, A. Further experimental investigation of rock weathering by salt and other mechanical processes. *Z. Fur Geomorphol. Suppl.* **1974**, *21*, 1–12.
43. Sperling, C.; Cooke, U. Laboratory simulation of rock weathering by salt crystallization and hydration processes in hot, arid environments. *Earth Surf. Process Landf.* **1985**, *10*, 541–555. [[CrossRef](#)]
44. Punuru, A.; Chowdhury, A.; Kulshreshtha, N.; Gauri, K. Control of porosity on durability of limestone at the great sphinx, Egypt. *Environ. Geol. Water Sci.* **1990**, *15*, 225–232. [[CrossRef](#)]

**Disclaimer/Publisher's Note:** The statements, opinions and data contained in all publications are solely those of the individual author(s) and contributor(s) and not of MDPI and/or the editor(s). MDPI and/or the editor(s) disclaim responsibility for any injury to people or property resulting from any ideas, methods, instructions or products referred to in the content.